ASTRONOMY & ASTROPHYSICS
SUPPLEMENT SERIES

Astron. Astrophys. Suppl. Ser. **92**, 473-480 (1992)

Optical CCD imaging of some Herbig *Ae/Be* stars

H.C. Bhatt and R. Sagar

Indian Institute of Astrophysics, Bangalore 560034, India

Received April 10; accepted June 17, 1991

Abstract. — We present results of *V*, *R* and Hα CCD imaging for 15 Herbig *Ae/Be* stars. Light variations of more than $\sim$ 2 mag in *V* have been noticed in stars T Ori, RR Tau and LHα 25. The nature of the variations in brightness and colour indicates that changes in the distribution of the circumstellar material around the stars could be the reason for the variability. For most of the objects, the observed radial variation of the surface brightness in different filters can be understood in terms of the light scattered by dust particles in the surrounding nebula with radially decreasing dust density. A bright emission knot located $\sim$ 14 arc sec north and 7 arc sec east of R Mon is found to be inexplicable in terms of scattering of central star light by nebular dust.

Key words: Herbig *Ae/Be* stars — photometry — morphology — CCD imaging.

1. Introduction.

Herbig *Ae/Be* stars (Herbig 1960) are recognized as early-type stars of intermediate mass ($\sim$ 3-4 $M_\odot$). These stars are characterized by emission lines and are often associated with dark nebulous material consisting of gas and dust (cf. Strom *et al.* 1972, Finkenzeller & Mundt 1984 and references therein). The stars generally illuminate fairly bright nebulosities in their immediate vicinity. While detailed studies by Strom *et al.* (1972) indicate that these stars are pre-main sequence (PMS) objects, Herbst *et al.* (1982) have suggested that these objects might be fast rotating main sequence stars.

Herbig *Ae/Be* stars generally show photometric variability and infrared excesses. Since these objects have circumstellar material, which may in fact be the cause of the variability, their photometric measurements should include the extended nebulous structure around them. Therefore imaging with charged coupled devices (CCDs) is better suited for this purpose. In this paper, we present results of such imaging in *V* and *R* photometric passbands and Hα 6563 filter for 15 *Ae/Be* stars. The coordinates and other general information about these stars are listed in Table 1. We derive photometric magnitudes for the central stars (within a circular aperture of 18 arc sec diameter) as well as the integrated magnitudes for the objects including their circumstellar nebulosities. The latter should be more meaningful measures of the luminosities of the central star. We have also studied the radial surface brightness distribution and colour gradient in these objects.

2. Observations and reductions.

The CCD images were obtained on the nights of 10/11 December 1988 and 11/12 February 1989 in the *V* and *R* photometric passbands and in Hα 6563 filter with band width (FWHM) of 160 Å using a blue coated Thomson-CSF TH 7882 CCD detector (576×384 pixel^2) at the *f*/13 Cassegrain focus of the 102 cm reflector located at the Vainu Bappu Observatory (VBO), Kavalur. The details of the CCD system as well as its photometric performance have been given by Sagar & Pati (1989). Briefly, each pixel on the CCD corresponds to 0.36 arc sec on the sky. Bias and dark frames were taken at regular intervals. Flat-field exposures were made using the twilight sky. The details of the observations of the programme stars are given in Table 2. The photoelectric sequence given by Christian *et al.* (1985) in the star cluster NGC 4147 was observed for the calibration purpose. They cover a range in brightness ($16.6 < V < 18.3$) as well as in colour ($-0.09 < (V - R) < 0.76$).

The data were reduced mainly at the VBO VAX 11/780 System using the STARLINK software package and the COMTAL Vision one image display station. Bias and dark subtraction and flat-field correction have been done in the usual manner. The uniformity of the flat-fields is better than a few percent in all the filters.

3. Results and discussion.

3.1. PHOTOMETRY.

The photometry of stars on the data frames has been done using an aperture of 50 pixels diameter ($\sim$ 18 arc sec) centred on the stars with the help of a programme written locally for the interactive data reduction on the COMTAL. The sky values have been estimated interactively using rectangular aperture on the data frames displayed on the COMTAL. Weighted average of several such measurements has been used as the sky value in determining the aperture magnitude of the programme stars. In filters where more than one set of CCD images have been taken, the aperture magnitudes have been averaged by taking into account the differences in exposure times and atmospheric extinction coefficients. In this as well as in the determination of zero-point of the CCD data frame, we have used the mean values of atmospheric extinction coefficients for the site.

The calibrated V, R photometric results for the programme stars have been listed in Table 3. Photometric magnitudes of another 3 stars namely V376 Cas, HI Ori and LkHα 213 have also been measured and given in Table 3, as they are located on the CCD images of the programme objects LkHα 198, HK Ori and LkHα 215 respectively. In converting the CCD magnitudes into the standard photometric system we have used colour equations given by Sagar & Pati (1989) for the present CCD system and zero-points determined by us with respect to the photoelectric sequence given by Christian *et al.* (1985) for the cluster NGC 4147. Since no calibration was available for Hα colours (R-Hα) listed in Table 3 are relative to star HD259431 ($\equiv$ MWC147) which showed no photometric variation on a time scale of years (cf. Breger 1974, Halbedel 1989). For this star the value of (R-Hα) has been normalized to zero. The magnitudes and colours have an uncertainty of $\sim$ 0.05 mag.

For all the stars except T Ori, RR Tau and HD 259431, the value of (R-Hα) is roughly constant (~ -1), whereas ($V-R$) colour shows a large variation from one object to another. The reason for the near constancy of (R-Hα) is perhaps the relatively large band width of the Hα filter used, so that the Hα filter acts effectively as a continuum filter adjacent to the R photometric passband except when the Hα emission is exceptionally strong which may be the case for T Ori, RR Tau and HD 259431.

3.1.1. *Photometric variability.*

A comparison of the present V and ($V-R$) values with those compiled by Herbig & Bell (1988) and given by Shevchenkov & Yakubov (1989) indicates that out of 18 stars listed in Table 3, only three; namely T Ori, RR Tau and LHα 25 showed large ($\geq$ 2 mag) variation in V. T Ori and RR Tau have become fainter and redder while LHα 25 has become brighter and bluer. Earlier studies have also found that the V magnitude of T Ori varies from 9.4 to 12.2 mag (Parenago 1952, 1954) and that of RR Tau varies from 12.3 to 14.5 mag (Kardopolov *et al.* 1989). The nature of the change in brightness and colour seems to be consistent with the idea that variation in circumstellar dust distribution could be responsible for the observed light variations. The extinction due to dust is accompanied by reddening so that stars are redder when they are fainter because of increased column density of dust along the line of sight.

Star LHα 25 (Walker 1956, star 90) has become brighter by $\sim$ 2.8 mag in V. To understand this change, we list in Table 4 previous photometric and spectroscopic measurements of the star from the literature. Variation in V of several hundredths of a magnitude in a few hours as well as large ($>$ 0.3 mag) long-term light variations have been observed in the star by earlier invertigators (cf. Walker 1956, Breger 1972, Mendoza & Gómez 1980, Pérez *et al.* 1987). Spectroscopic measurements indicate the apparent evolution toward earlier spectral types for this star. A change in spectral type from A2-A3 to B1-1.5 (see Table 4) corresponds to $\sim$ 4 mag brightening in the absolute V magnitude of the star which is about 1 mag smaller than the brightening observed by us in V passband. Optical, ultraviolet, infrared and polarization observations of the star indicate that it is embedded in an optically-thick circumstellar dust shell leading to optical extinction as well as infrared excess in ($V-L$) of several magnitudes (cf. Strom *et al.* 1972, Breger 1974, Rydgren 1977, Warner *et al.* 1977, Sitko *et al.* 1984). The observed increase in brightness might be due to an expansion of the circumstellar shell with a resulting drop in dust-particle column density in the line of sight as suggested earlier by Breger (1972) and Mendoza & Gómez (1980). To confirm this scenario, further optical, infrared and polarimetric observations are required.

The star LHα 25 has a proper motion membership probability of 92% for the galactic open star cluster NGC 2264 (cf. Vasilevskis *et al.* 1965). Observations at different wavelengths indicate that this star is a PMS object surrounded by an optically thick circumstellar shell. Consequently, it lies well below the main-sequence in the $V,(B-V)$ colour magnitude diagram of the NGC 2264 (cf. Sagar & Joshi 1983). The present V magnitude i.e. brightening of the star moves its position close to the main-sequence but is still $\sim$ 2 mag fainter than the brightness predicted by Strom *et al.* (1972) on the basis of surface gravity determination. In the light of these discussions, we conclude that this star is presently at an interesting phase of PMS stellar evolution. Its further observations will improve significantly our knowledge of PMS stellar evolution.

It should also be noted here that the cause of most of the activity in young stellar objects like the Herbig Ae/Be stars may be the circumstellar accretion disks that

could still be surrounding the central objects. Variation in the accretion rate could then result in the observed photometric variability.

3.1.2. *Integrated brightness of the nebulae.*

Integrated magnitude and colour of the stars associated with nebulae are also listed in Table 3. Except in the case of LkHα 198 and R Mon, integrated $(V-R)$ colour does not differ significantly from the $(V-R)$ colour of the associated star. In these cases colour has become bluer. The integrated V magnitude has become significantly brighter ($\geq$ 0.4 mag) in the cases of LkHα 198, V376 Cas, V380 Ori, LkHα 208, LkHα 215 and R Mon. As expected, brightenning is more for those objects in which extended nebulosities are present (cf. Sect. 3.2). This is further supported by the fact that brightenning is positively correlated with the value of A_v (see Tables 1 and 3), a major part of which may be due to circumstellar dust.

3.2. NEBULAR STRUCTURE.

In order to see the nebulous features around the stars, we inspected the CCD images on the COMTAL and found that BD + 61° 154, AB Aur, HK Ori, HD 259431, LHα 25 and HD 53367 do not show any nebulous feature while LkHα 198, V376 Cas, T Ori, V380 Ori, RR Tau, HD 250550, LkHα 208, LkHα 215, R Mon and Z CMa show extended nebulosities either on one or more CCD images. Nebulosities are more pronounced in Hα and R than in V. The Hα and R images are very similar except in the case of T Ori. The relatively large band width of the Hα filter and its proximity to the R passband may be responsible for the similarity of the images in these bands. To illustrate the extent of the nebulosities, we therefore present contour maps only in R filter and they are shown in Figure 1. Contours have generally been drawn for 4 intensity levels. The lowest intensity level for the contour is taken as $\sim 3\ \sigma$ above the mean sky level. The mean and standard deviation, σ, are evaluated from the sky values determined at 10-15 different places using rectangular aperture on the CCD image displayed on the COMTAL. Higher intensity levels are taken arbitrarily. The innermost and the outermost contours represent the highest and the lowest intensity levels respectively and those lying in between them correspond to the intermediate intensity levels with the intensity decreasing radially from the central star.

3.2.1. *Radial brightness and colour distribution.*

Emission from the circumstellar nebula derives its energy from the central stars. The radial variation of the nebular emission therefore depends on the density distribution of the circumstellar material. We have plotted the surface brightness S in relative magnitudes $S(m)$, within circular annuli with different radii *versus* the radial distance from the exciting star. Figure 2 shows such a plot for V380 Ori in R filter. The surface brightness falls with radius R. A fit of the form $S\alpha R^{-x}$ has been made and the values of x evaluated from the distribution of surface brightness in different filters are given in Table 5. The values of x range from $\sim$ 1.5 to $\sim$ 3.0. For a given object the value of x in different filters is the same within the errors except T Ori which perhaps has a strong Hα emission from its surrounding nebulosity. If the nebular emission is due to scattering of light from the central star by dust in the nebula, then for a spherically symmetric dust distribution with uniform density the expected value of x would be 1. This follows from the inverse square drop in the incident radiation from the central star and line of sight integration. The observed values of x therefore indicate a radial distribution of dust density ρ which is falling with R. For a ρ distribution of the form $\rho(R)\alpha R^{-y}$ in an optically thin nebula the value of x would be $y+1$. For the observed nebulae (see Table 5) the value of y thus ranges from $\sim$ 0.5 to $\sim$ 2.

The colour of the dust scattered light will become bluer with increasing R because of stronger scattering at shorter wavelengths. This is in agreement with the observed variation of colour $(V-R)$ with radial distance from central star (see Fig. 3) for most of the objects. In optically thick nebulae the extinction within the nebulae can cause the central star light to drop off with radial distance faster than inverse square and also make it relatively redder. This may increase the value of x and cause reddening of the colour $(V-R)$ with increasing radial distance. This may be the case for LkHα 208 and LkHα 215. For T Ori there is extensive Hα nebulosity around the star which makes the R magnitude relatively brighter and consequently cause a steep rise in the $(V-R)$ colour with increasing radial distance as seen in Figure 3.

3.2.2. *Polarization and morphological characteristics.*

Polarimetric observations for 8 of our objects have been carried out by Jain *et al.* (1990) within a few months of the present observations. So we have used them to study the correlation between polarization and asymmetry paramater (a/b) defined as the ratio of the major axis to the minor axis of the contours within a circular aperture of 18 arc sec diameter. A circularly symmetric image has $a/b = 1$ and deviations from this value indicate asymmetry. We list the values of (a/b) and linear polarization p, for R filter in Table 6 which clearly shows that stars showing larger asymmetry tend to have larger degree of polarization. Two stars namely HD 250550 and 259431 have almost symmetrical structure but have linear polarization $\sim$ 1% which may be due to interstellar dust and/or asymmetric circumstellar dust distribution very close to the central star that is not apparent in the large scale images.

3.2.3. *Nebulous feature associated with R Mon.*

Brugel *et al.* (1984) found narrow [SII] line emission regions on opposite sides of R Mon, at an angular distance of about 10 arc sec from it along a line joining R Mon and HH 39. Infrared images of R Mon and its associated nebula have been found to contain a number of structures e.g. emission knots and a narrow jet (Aspin *et al.* 1985, 1988). In Figure 4, we present the CCD images of this object in R filter. Apart from other morphological details, we note the presence of an exceptionally bright region of emission $\sim$ 14 arc sec north and 7 arc sec east of R Mon. This feature is distinct from those found by Brugel *et al.* (1984). We have measured the brightness of this feature within a number of concentric circular apertures and obtained $R = 13.13$ mag and $V - R = 0.37$ mag in an aperture of radius 5 arc sec. Increasing the aperture radius to 7 arc sec increases the brightness only to $R = 12.6$ mag. If this feature (a region of diameter $\sim$ 10 arc sec) is a density enhancement in the nebular dust, scattering the central star light, the expected brightness at a radial distance of $\sim$ 16 arc sec from the central star assuming 50% albedo and no internal extinction due to dust is $\sim$ 4.7 mag fainter than the central star. However, the observed magnitude difference in R is only 1.8 mag. If we use the integrated magnitude for the entire complex of the central star plus the nebula ($R = 10.0$ mag) the magnitude difference is still only 3.1 mag. In V and Hα also the magnitude differences are nearly the same. This may suggest that the emission from this feature is not simply the light scattered from the central star but there is an intrinsic source of radiation within the feature. This may be due to line emission from ionised gas in this region or there may be an additional embedded star. Spectroscopic observations may reveal line emission from this region if there is such emission and any embedded stellar source would make this feature a strong source of far infrared radiation. Further observations are required to understand the nature of this feature.

4. Conclusions.

We have presented results of CCD imaging in V and R photometric passbands and Hα 6563 filter for 15 Herbig Ae/Be stars. Photometric magnitudes for the central stars as well as integrated brightness of their surrounding nebulae have been evaluated. The main conclusions of the present work are:

(i) Large photometric variations (> 2 mag in V) have been found in T Ori, RR Tau and LHα 25. The variability in brightness has been found to be correlated with colour variations i.e. the colour becomes bluer if the star brightens and redder if it fades. This is consistent with the idea that changes in the circumstellar dust distribution cause these variations.

(ii) The star LHα 25 is a proper motion member of the galactic star cluster NGC 2264. Its brightening and bluing has moved the star's position from well below the main-sequence to close to it in the colour-magnitude diagram of the cluster.

(iii) The radial variation of surface brightness and colour has been studied. The dust density is inferred to fall off with radial distance from the central star.

(iv) LkHα 198, V376 Cas, T Ori, V380 Ori, RR Tau, HD 250550, LkHα 208, LkHα 215, R Mon and Z CMa show presence of extended nebulosities around the central stars. Asymmetry in the morphology of the nebulae around the central stars appears to be correlated with the degree of polarization.

(v) Photometric measurements of a bright feature located $\sim$ 14 arc sec north and 7 arc sec east of R Mon indicate that there is an intrinsic source of radiation within the feature. Further observations are required to understand the nature of this feature.

Acknowledgements.

We thank Y.D. Mayya for allowing us to use his programmes for the data reductions.

References

Aspin C., McLean I.S., Coyne G.V. 1985, A&A 149, 158
Aspin C., McLean I.S., Rayner J.T., Mc Caughrean M.J. 1988, A&A 197, 242
Breger M. 1972, ApJ 171, 539
Breger M. 1974, ApJ 188, 53
Brugel E.W., Mundt R., Bührke T. 1984, ApJL 287, L73
Christian C.A., Adams M., Barnes J.V., Butcher H., Hayes D.S., Mould J.R., Siegel M. 1985, PASP 97, 363
Finkenzeller U., Mundt R. 1984, A&AS 55, 109
Halbedel E.M. 1989, PASP 101, 1004
Herbst W., Miller D.E., Warner J.W., Herzog A. 1982, AJ 87, 98
Herbig G.H. 1954, ApJ 119, 483
Herbig G.H. 1960, ApJS 4, 337
Herbig G.H., Bell K.R. 1988, Lick Obs. Bull. No. 1111
Jain S.K., Bhatt H.C., Sagar R. 1990, A&AS 83, 237
Kardopolov V.I., Tilip'ev G.K., Shaimieva A.F., Shutemova N.A. 1989, SvA 65, 489
Mendoza E.E., Gómez T. 1980, MNRAS 190, 623
Parenago P. 1950, Variable Stars 7, 169
Parenago P. 1954, Publ. Sternberg Astr. Inst. 25, 214
Pérez M.R., Thé P.S., Westerlund B.E. 1987, PASP 99, 1050

Rydgren A.E. 1977, PASP 89, 823
Sagar R., Joshi U.C. 1983, MNRAS 205, 747
Sagar R., Pati A.K. 1989, BASI 17, 6
Shevchenko V.S., Yakubov S.D. 1989, SvA 33, 370
Sitko M.L., Simon T., Meade M.R. 1984, PASP 96, 53
Strom S.E., Strom K.M., Brooke A.L., Bregman J., Yost J. 1972, ApJ 171, 267
Vasilevskis S., Sanders W.L., Blaz A.G.A.Jr. 1965, AJ 70, 797
Walker M.F. 1956, ApJS 2, 365
Warner J.W., Strom S.E., Strom K.M. 1977, ApJ 213, 427
Young A., 1978, PASP 90, 144

TABLE 1. *General information about the programme stars. α, δ and galactic coordinates are from Herbig & Bell (1988). The A_v and distance values of LkHα 198 are based on the observations by Shevchenko & Yakubov (1989) while for others they have been taken from Finkenzeller & Mundt (1984).*

Star	Other designation	α_{1950} h	m	s	δ_{1950} o	'	"	l	b	A_v (mag)	Distance (pc)
LkH$_\alpha$ 198	V633 Cas	00	08	47.45	+58	33	05.2	117.8	-3.6	3.6	630
BD +61° 154	V594 Cas, MWC 419	00	40	21.94	+61	38	15.1	122.0	-0.9	2.2	650
AB Aur	BD +30° 741, HD 31293	04	52	34.24	+30	28	21.9	172.5	-8.0	-	160
HK Ori	MH$_\alpha$ 265-13, MWC 497	05	28	40.08	+12	07	00.2	192.6	-11.6	1.5	460
T Ori	P2247, MWC 763	05	33	23.05	-05	30	25.9	209.2	-19.3	1.1	460
V380 Ori	BD -6° 1253, P2393	05	33	59.50	-06	44	46.4	210.4	-19.7	1.5	460
RR Tau	AS 103	05	36	23.84	+26	20	49.2	181.5	-2.5	2.5	800
HD 250550	MWC 789	05	59	06.43	+16	30	59.4	192.6	-3.0	0.3	700
LkH$_\alpha$ 208		06	04	53.17	+18	39	55.0	191.4	-0.8	1.9	2000
LkH$_\alpha$ 215		06	29	56.10	+10	11	24.0	201.8	0.5	2.5	800
HD 259431	MWC 147	06	30	19.40	+10	21	38.0	201.7	0.7	1.4	800
R Mon	BD +8° 1427,MWC 151	06	36	26.05	+08	46	54.5	203.8	1.3	2.8	800
LH$_\alpha$ 25	V590 Mon	06	37	59.49	+09	50	53.4	203.0	2.1	0.9	800
Z CMa	HD 53179,MWC 166	07	01	22.52	-11	28	36.0	224.6	-2.6	-	1150
HD 53367	MWC 166, IC 2177	07	02	02.00	-10	24	36.0	-	-	2.3	1150

TABLE 2. *Details of observations.*

Object	Filter	Exposure time (in seconds)	Date
LkH$_\alpha$ 198	V	300	10/11 Dec 1988
	H$_\alpha$	720,1200	"
	R	300	"
BD 61° 154	V	120	"
	H$_\alpha$	600	"
	R	1200	"
AB Aur	V	60,10	"
	H$_\alpha$	300	"
	R	60,120	"
HK Ori	V	120	"
	H$_\alpha$	900	"
T Ori	V	60	"
	H$_\alpha$	300	"
	R	60	"
V380 Ori	V	60	"
	H$_\alpha$	60,300	"
	R	30,120	"
RR Tau	V	180	"
	H$_\alpha$	900	"
	R	300	"
HD 250550	V	180	"
	H$_\alpha$	600	"
	R	120	"
LkH$_\alpha$ 208	V	300	"
	H$_\alpha$	900	"
	R	300	"
LkH$_\alpha$ 215	V	120	"
	H$_\alpha$	300	"
	R	60,120	"
HD 259431	V	30	11/12 Feb 1989
	H$_\alpha$	60	"
	R	10	"
R Mon	V	60	"
	H$_\alpha$	120,120	"
	R	10,30,30	"
LH$_\alpha$ 25	V	15	"
	H$_\alpha$	120	"
	R	15	"
Z CMa	V	30	"
	H$_\alpha$	120	"
	R	10	"
HD 53367	V	10	"
	H$_\alpha$	30	"

TABLE 3. *V, R and Hα magnitudes of the programme stars and integrated I(V), I(V−R) magnitudes of stars plus nebulae.*

Star	V (mag)	(V-R) (mag)	(R-H$_\alpha$) (mag)	I(V) (mag)	I(V-R) (mag)
LkH$_\alpha$ 198	14.00	0.83	-1.00	12.93	0.07
V376Cas	14.99	0.81	-1.04	14.40	0.96
BD +61° 154	10.41	0.43	-0.94	-	-
AB Aur	7.05	0.12	-1.31	-	-
HK Ori	11.91	-	-	-	-
HI Ori	13.56	-	-	-	-
T Ori	12.50	0.40	0.91	12.48	0.54
V380 Ori	10.53	0.54	-0.84	9.78	0.37
RR Tau	13.33	0.72	-0.57	13.11	0.72
HD 250550	9.50	-0.02	-0.87	9.42	-0.03
LkH$_\alpha$ 208	11.67	0.28	-1.19	11.29	0.20
LkH$_\alpha$ 215	10.46	0.40	-1.01	10.06	0.47
LkH$_\alpha$ 213	15.18	0.87	-	-	-
HD 259431	8.72	0.29	0.00	-	-
R Mon	11.88	0.60	-0.75	10.36	0.27
LH$_\alpha$ 25	9.70	0.08	-1.26	-	-
Z CMa	9.56	0.87	-1.27	9.46	0.81
HD 53367	7.10	-	-	-	-

TABLE 4. *Photometric and spectroscopic measurements of LHα 25.*

Period	V (mag)	(U-B) (mag)	(B-V) (mag)	(V-R) (mag)	References
1951 - 1953	14.0	-	-	-	Herbig (1954)
Jan - Feb 1954	13.18 to 12.88	0.08 to -0.06	0.22 to 0.15	-	Walker (1956)
Dec 1969	12.72 to 12.65	-	-	-	Breger (1972)
Dec 1970	12.56 to 12.50	-0.19 to -0.20	0.17 to 0.15	-	Breger(1972)
1970 - 1971	12.50	-	-	-	Strom et al. (1972)
1971	12.53	-	-	-	Breger (1974)
1973	12.62	-	-	-	Breger (1974)
1975	12.78	0.02	0.15	0.44	Mendoza & Gómez (1980)
1977	12.48	-	-	-	Mendoza & Gómez (1980)
	12.80	-	0.17	0.32	Rydgren (1977)
1978	12.76	0.08	0.14	-	Sagar & Joshi (1983)
1980 - 1981	12.84 to 12.91	-	-	-	Sitko et al. (1984)
1984 - 1986	12.64	-0.20	0.16	0.23	Pērez et al. (1987)
Feb 1989	9.70	-	-	0.08	Present

Spectroscopic measurements

Spectral type	Reference
A2 - A3	Herbig (1954)
A2p	Walker (1956)
B8 + shell	Herbig (1960)
B9-A0	Warner et al. (1977)
B4 V	Young (1978)
B8pe V	Pērez et al. (1987)
B5 V	Pērez et al. (1987)
B1-1.5 V	Joner quoted by Pērez et al. (1987)

TABLE 5. *The values of the power index x in the radial variation of surface brightness of the programme stars.*

Star	x (±error) in filter		
	V	Hα	R
LkH$_\alpha$ 198	1.9±0.04	1.6±0.04	1.8±0.05
V376Cas	1.5±0.08	1.2±0.05	1.4±0.06
T Ori	2.8±0.19	1.9±0.13	2.3±0.10
V380 Ori	1.7±0.05	1.8±0.06	1.8±0.05
RR Tau	2.7±0.08	2.8±0.09	2.9±0.12
HD 250550	2.8±0.09	2.9±0.17	3.2±0.18
LkH$_\alpha$ 208	1.8±0.06	1.9±0.07	1.9±0.10
LkH$_\alpha$ 215	2.0±0.12	2.1±0.12	1.9±0.17
HD 259431	2.4±0.05	2.6±0.06	2.6±0.07
R Mon	1.6±0.08	1.5±0.10	1.5±0.11
Z CMa	2.7±0.10	3.0±0.15	3.1±0.10

TABLE 6. *Asymmetry parameter (a/b) for the stars having linear polarization (p) measurements by Jain et al. (1990). The values are for R filter.*

Star	(a/b)	p in %
AB Aur	1.0	0.10±0.04
T Ori	1.0	0.12±0.05
V380 Ori	1.4	0.55±0.06
HD 250550	1.0	1.00±0.05
LkH$_\alpha$ 215	1.3	1.00±0.06
HD 259431	1.0	0.91±0.04
Z CMa	1.3	0.79±0.04
HD 53367	1.0	0.23±0.04

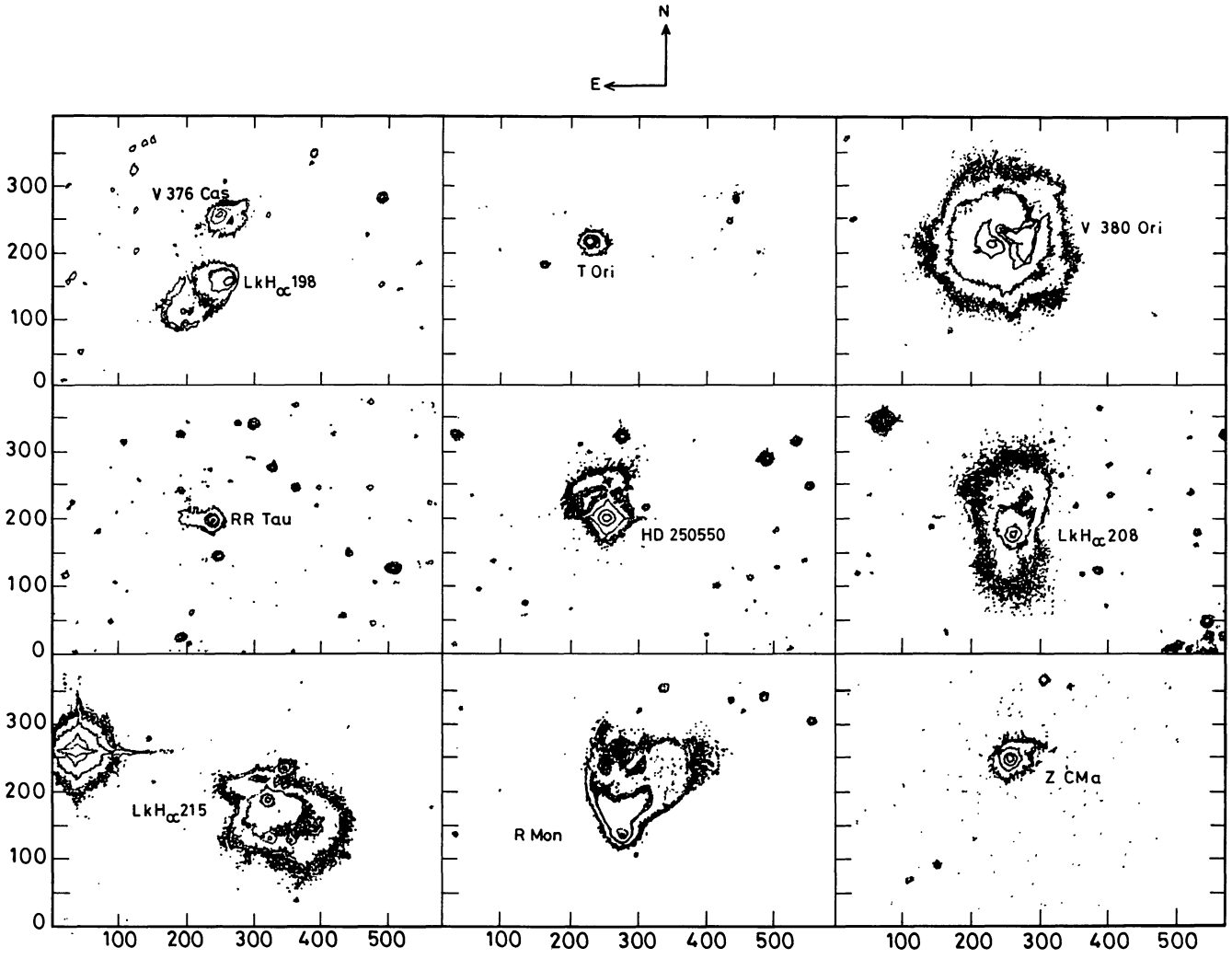

FIGURE 1. Contour maps reproduced from the CCD images in *R* filter are for the objects showing extended nebulosities around the central star. Coordinates of both axes are in units of pixels. Exposure times are 300, 60, 120, 300, 120, 300, 60, 30 and 10 seconds for the stars LkHα 198, T Ori, V380 Ori, RR Tau, HD 250550, LkHα 208, LkHα 215, R Mon and Z CMa respectively. Count levels of the contours are 35, 50 and 200 for LkHα 198; 5, 15, 50, 100 and 1000 for T Ori; 12, 20, 100 and 1000 for V380 Ori; 30, 50, 100 and 2000 for RR Tau; 13, 20, 100 and 1000 for HD 250550; 31, 40, 100 and 1000 for LkHα 208; 8, 15, 100 and 1000 for LkHα 215; 9, 15, 100 and 500 for R Mon and 5, 12, 100 and 1000 for Z CMa. The innermost and the outermost contours represent the highest and the lowest intensity levels respectively.

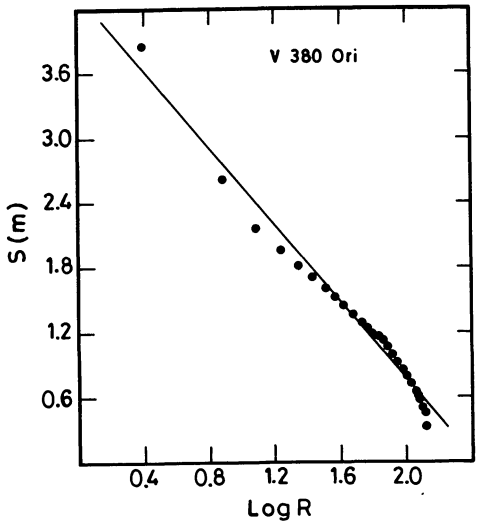

FIGURE 2. Variation of surface brightness in relative magnitudes $S(m)$, with radial distance R in pixels is shown for V380 Ori in R filter. The solid line represents the best fit straight line through the data points using least-squares solution.

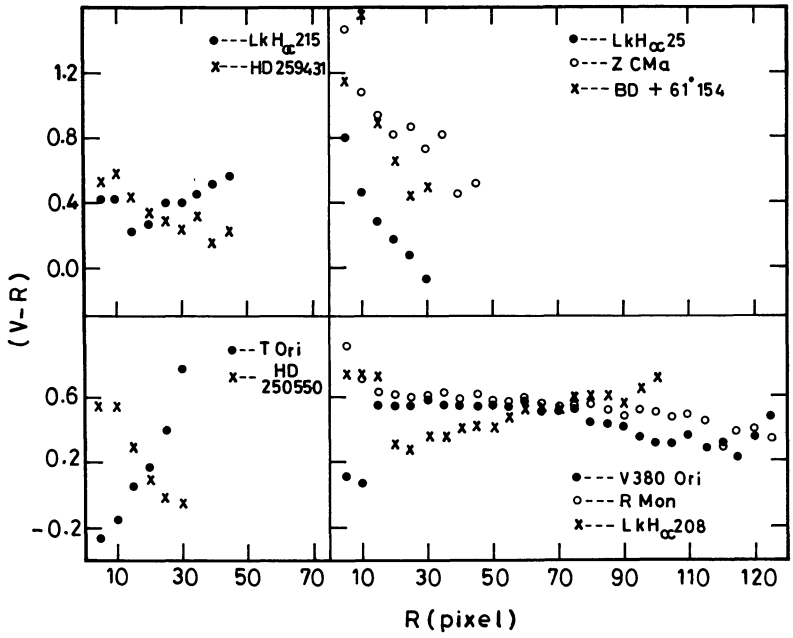

FIGURE 3. Plot of colour $(V - R)$ in magnitude *versus* radial distance R in pixel from the central star.

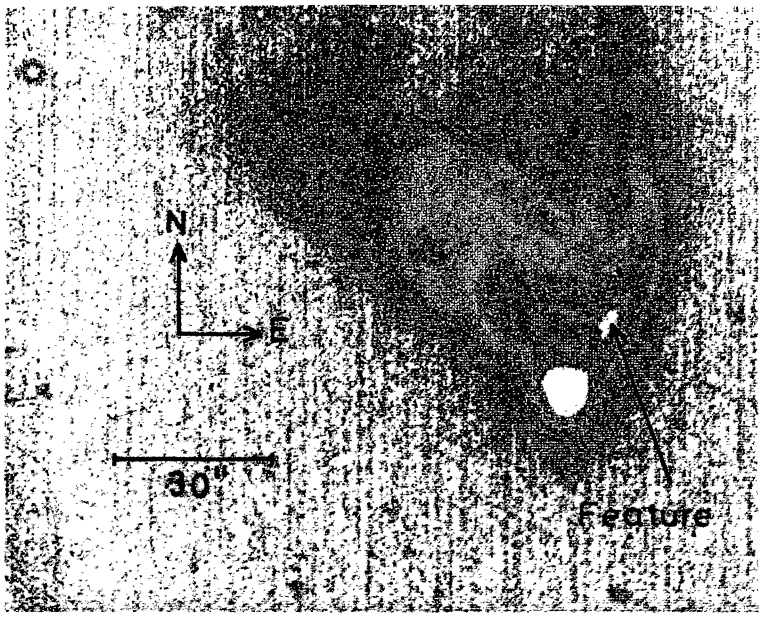

FIGURE 4. CCD image of R Mon in R filter. The exceptionally bright feature located ~ 14 arc sec north and ~ 7 arc sec east of R Mon is marked.